JACS
JOURNAL OF THE AMERICAN CHEMICAL SOCIETY
pubs.acs.org/JACS
Article

Evidence for Dearomatizing Spirocyclization and Dynamic Effects in the Quasi-stereospecific Nitrogen Deletion of Tetrahydroisoquinolines

Jeanne Masson-Makdissi,[‖] Remy F. Lalisse,[‖] Mingbin Yuan,[‖] Balu D. Dherange, Osvaldo Gutierrez,* and Mark D. Levin*

Cite This: J. Am. Chem. Soc. 2024, 146, 17719−17727
Read Online
ACCESS | Metrics & More | Article Recommendations | Supporting Information

ABSTRACT: Selectivity in organic chemistry is generally presumed to arise from energy differences between competing selectivity-determining transition states. However, in cases where static density functional theory (DFT) fails to reproduce experimental product distributions, dynamic effects can be examined to understand the behavior of more complex reaction systems. Previously, we reported a method for nitrogen deletion of secondary amines which relies on the formation of isodiazene intermediates that subsequently extrude dinitrogen with concomitant C−C bond formation via a caged diradical. Herein, a detailed mechanistic analysis of the nitrogen deletion of 1-aryl-tetrahydroisoquinolines is presented, suggesting that in this system the previously determined diradical mechanism undergoes dynamically controlled partitioning to both the normal 1,5-coupling product and an unexpected spirocyclic dearomatized intermediate, which converges to the expected indane by an unusually facile 1,3-sigmatropic rearrangement. This mechanism is not reproduced by static DFT but is supported by quasi-classical molecular dynamics calculations and unifies several unusual observations in this system, including partial chirality transfer, nonstatistical isotopic scrambling at the ethylene bridge, the isolation of spirocyclic dearomatized species in a related heterocyclic series, and the observation that introduction of an 8-substituent dramatically improves enantiospecificity.

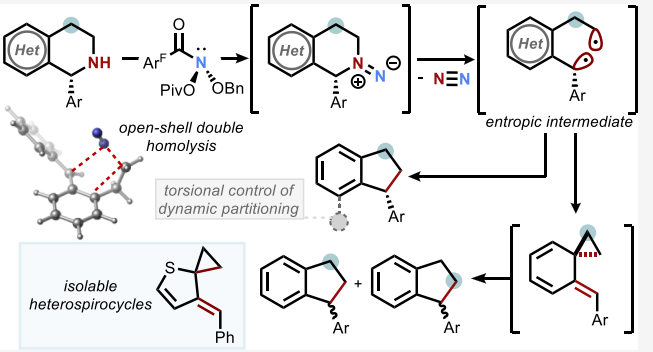

INTRODUCTION

Facile access to the isodiazene-reactive intermediate directly from secondary and primary amines has greatly expanded the ability to productively deploy nitrogen deletion as a synthetic procedure. Several recent contributions have offered one- or two-step procedures as an entry to these transformations (Figure 1A),[1−9] adding to the classical mechanistic studies which established the fundamentals of these reactive species and provided a bedrock for subsequent work.[10−22] As a prototypical skeletal edit, the continued development of nitrogen deletion and an understanding of its accompanying mechanism(s) are of critical importance to this growing field.[23] In particular, the complexity of substrates that can be examined has increased meaningfully with the introduction of mild methods that improve upon the functional group tolerance and laborious features of classical approaches, with an ensuing examination of scaffolds that had been previously not been subjected to scrutiny.[1,24−26] One persistent feature of all studies to date is that the geminate diradical pair formed upon N_2 extrusion from the isodiazene couples exceptionally quickly, such that even bond rotation processes do not intervene and stereospecificity is observed (Figure 1B).

RESULTS AND DISCUSSION

In that vein, we were initially perplexed to observe significant erosion of enantiopurity in the reaction of enantiopure tetrahydroisoquinoline (*S*)-**1a** with anomeric amide reagent **2**, affording the corresponding indane product **3a** in 69:31 e.r. (Figure 2A). While we first assumed that racemizing bond rotation in the intervening diradical was responsible for this low stereospecificity (noting that the prior art had neither examined 1,5-diradicals nor such electronically asymmetric substrates), our subsequent observations in this system as detailed herein have indicated that this seemingly simple result belies an unusual level of underlying complexity. Our first hint in this mechanistic puzzle was the isolation of the dearomatized spirocycle **5a** upon subjection of the analogous

Received: February 19, 2024
Revised: June 5, 2024
Accepted: June 7, 2024
Published: June 20, 2024

https://doi.org/10.1021/jacs.4c02491
J. Am. Chem. Soc. 2024, 146, 17719−17727

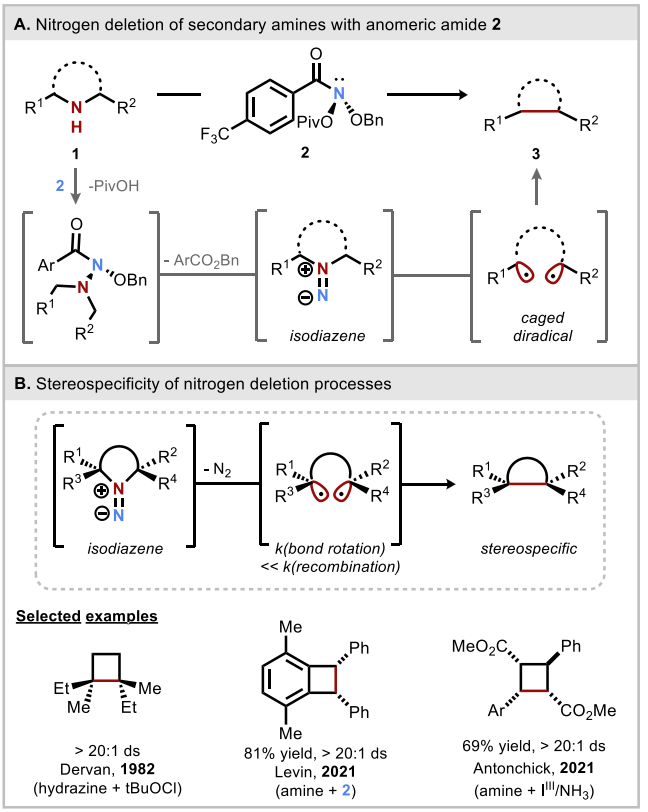

Figure 1. Mechanism and stereospecificity in nitrogen deletion reactions.

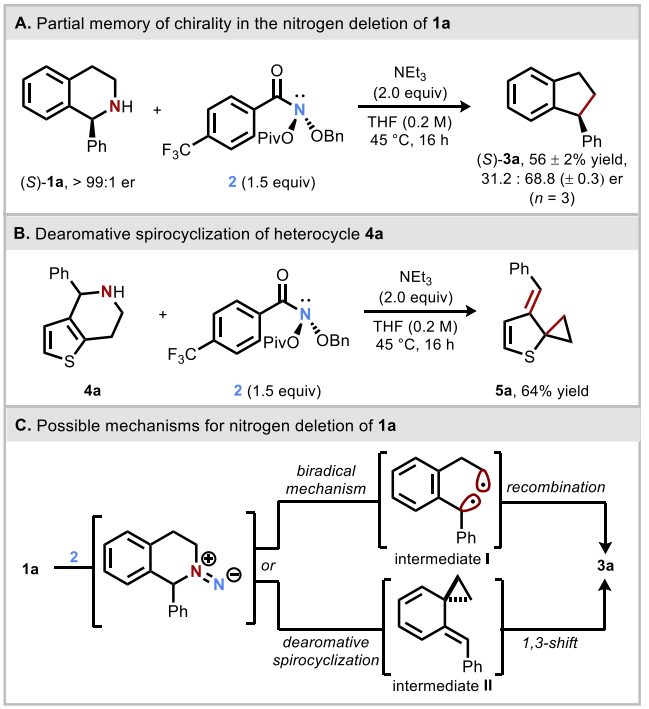

Figure 2. Interrogating an alternative mechanism for the nitrogen deletion of 1-aryl-tetrahydroisoquinolines.

tetrahydrothienopyridine **4a** to the same reaction conditions (Figure 2B).[27] The subversion of the normal nitrogen deletion pathway in this heterocyclic system suggested that an analogous process via intermediate **II** may likewise be operative in the benzenoid series (Figure 2C) and spurred further investigation.

Initial Experiments. We first validated that the spirocycle **5a** was competent to form the analogous cyclopenta[*b*]-thiophene **6a** (Figure 3A). Upon thermolysis in toluene at 100 °C, 1,3-rearrangement was observed in 96% yield. Monitoring of the reaction rate at a series of temperatures allowed extraction of the activation parameters ($\Delta H^{\ddagger}$ = 33.3 kcal/mol and $\Delta S^{\ddagger}$ = 12.7 cal/mol·K) as well as estimation of the $\Delta G^{\ddagger}_{298K}$ at 29.5 kcal/mol. This is in good agreement with the density functional theory (DFT) calculated barrier (an unrestricted calculation, with spin contamination addressed using the Yamaguchi correction) of 25.0 kcal/mol for a stepwise pathway for this transformation involving initial homolysis of the cyclopropane C−C bond, followed by rapid C−C bond formation (Figure 3B).[28,29] The alternative concerted 1,3-shift, in accordance with Woodward−Hoffmann analysis, is predicted to be prohibitively high in energy (~11 kcal/mol higher than the stepwise process). This is further consistent with previous observations of the thermal vinyl cyclopropane−cyclopentene rearrangement, though we note that the present example is far more facile than known analogues of this transformation in neutral systems.[30−36] This unusually facile 1,3-rearrangement lends credence to the competency of intermediate **II**.

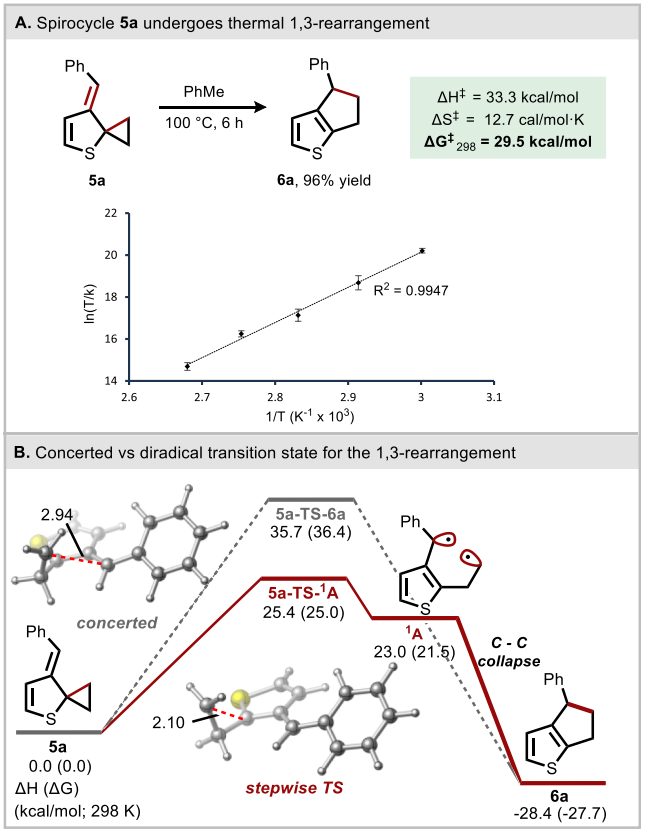

Figure 3. Eyring analysis for the rearrangement of spirocycle **5a**, *n* = 3, for each point. DFT at the UB3LYP-D3/def2TZVPP-SMD-(PhMe)//UB3LYP-D3/6-31G(*d*)-SMD (PhMe) level. Corrections to the single-point energies for the open-shell singlet geometries were made with the Yamaguchi correction (Table S6).

We next conducted an isotope labeling study with 3,3-d_2-**1a** to probe the intermediacy of a symmetric cyclopropane

https://doi.org/10.1021/jacs.4c02491
J. Am. Chem. Soc. 2024, 146, 17719−17727

intermediate and observed incorporation of the deuterium label into *both* the 2- and 3-positions of the indane product in a 64:36 ratio (Figure 4A). To further bolster this observation, we

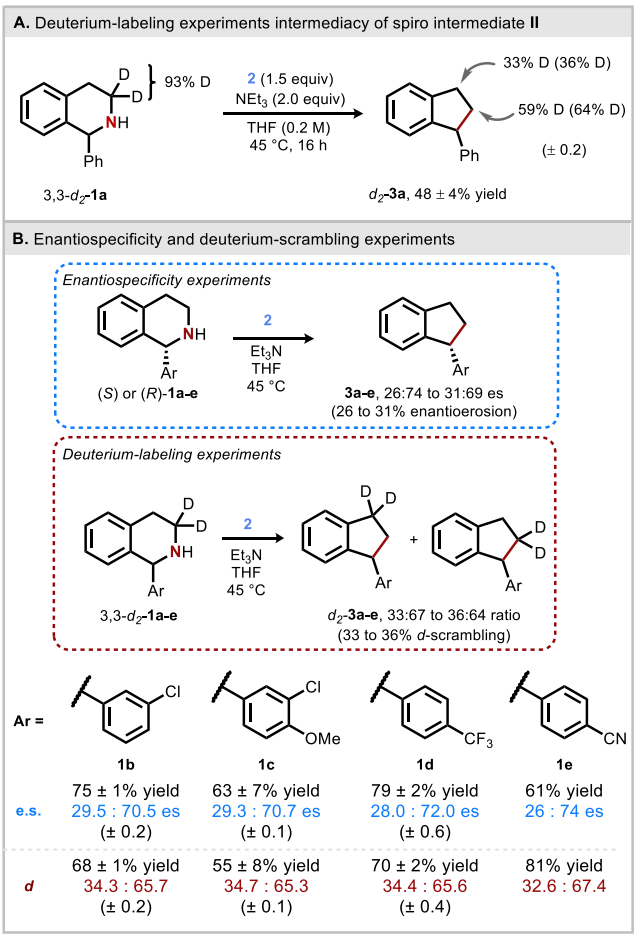

Figure 4. Enantiospecificity and deuterium-labeling studies. Values in parentheses are corrected for unlabeled starting material. $n = 3$ except for **1e**.

repeated both the enantiospecificity measurements and the deuterium incorporation experiments in triplicate for a small series of substituted tetrahydroisoquinolines (**1a**–**1e**) and observed consistent nonstatistical ratios across the board (Figure 4B).

While this provided the strongest experimental evidence yet for the intermediacy of the putative spirocycle **II**, we were struck by the nonstatistical ratios. While a kinetic isotope effect (KIE) could in principle explain the divergence from 50:50 in the deuterium labeling experiments, a symmetric intermediate such as **II** would be expected to undergo rearrangement to give a racemic material. This partial memory-of-chirality argues against a simplistic model in which the reaction proceeds only though an achiral intermediate such as **II**. We thus considered alternative explanations—either **II** must present some subtle element of chirality, or it is not the only relevant intermediate.

Helical Chirality Hypothesis. The above discussion was predicated on the intermediacy of the trans isomer of intermediate **II**, which is achiral. However, we reasoned that the corresponding cis isomer might display some degree of helical chirality (Figure 5A).[37−39] This proposition was based on our observations in the heteroaromatic series of substrates

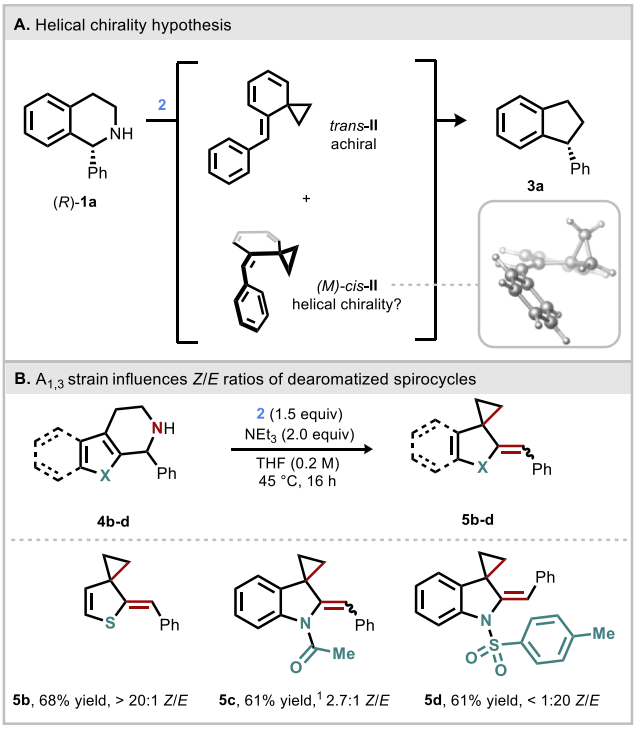

Figure 5. Probing helical chirality of the cis spiro intermediate **II**.[1] Yield of *Z* isomer.

(Figure 5B). Whereas thiophene substrate **5b** exclusively afforded a spirocycle with *Z* olefin geometry (c.f. **5a**), we found that an *N*-acyl-indole substrate (**5c**) afforded a mixture of olefin isomers, and further increase in the size of the *N*-substituent to toluenesulfonyl (**5d**) led to the exclusive formation of the *E* isomer.[40]

Given the differing steric profile of the 5- and 6-membered ring fusions, we conjectured that the benzenoid systems may be generating a mixture of cis- and trans-spirocyclic intermediates, with the former displaying helical chirality that may be responsible for the partial transfer of chiral information. To further test this hypothesis, we prepared substrate (*R*)-**1f**, wherein 8-methyl substitution was expected to engender a greater preference for *cis*-**II**, in analogy to the indole series. In the event, we observed a 95:5 e.r. in the isolated indane product, in accordance with our hypothesis (Figure 6A). A deuterium-labeling experiment with 3,3-d_2-**1f** showed similarly low deuterium scrambling (Figure 6B).

Perplexingly, while this new set of experiments was suggestive of the intermediacy of *cis*-**II** in the reaction of **1a**, DFT calculations did not support this premise (Figure 7). The isodiazene derived from substrate **1f** was predicted to proceed via barriers for irreversible formation of the cis and trans isomers that were isoenergetic, inconsistent with an exclusive cis pathway generating the observed, high enantiospecificity [**trans-TS-1(Me)** vs **cis-TS-1(Me)**]. In addition, the putative cyclic vinyl cyclopropane intermediates [***trans*-II(Me)** and ***cis*-II(Me)**] were also nearly isoenergetic demonstrating that, unlike **5b**–**5d**, the steric clash of the aryl substituent with either the Me or cyclopropane cancel out. While one might ascribe this inconsistency to a systematic computational error, the predicted rate of enantiomerization of cis spirocycle ($\mathbf{TS}_{rot}^{1/2}$, Figure 7) was substantially faster than its subsequent stepwise 1,3-rearrangement [via initial C−C bond homolysis

https://doi.org/10.1021/jacs.4c02491
J. Am. Chem. Soc. 2024, 146, 17719−17727

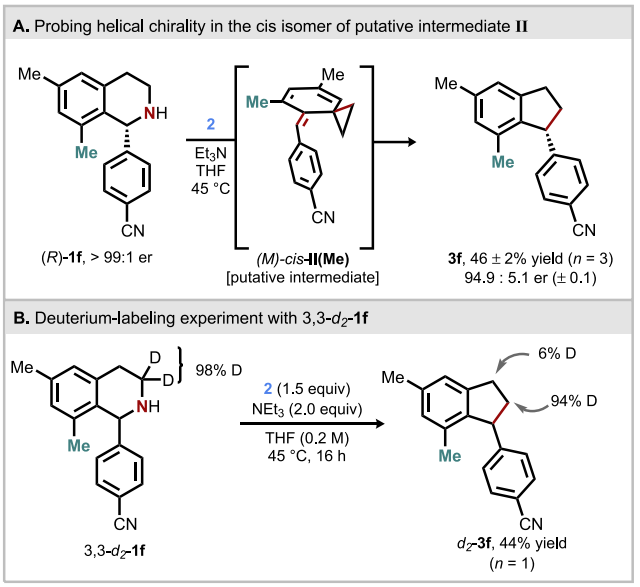

Figure 6. Probing helical chirality of the cis spiro intermediate **II**.

through **cis-II(Me)-TS-4**] to afford indane **3f**, further arguing against chirality transfer via the cis-spirocycle. Moreover, in the parent substrate, the barrier for the concerted process to form the cis spirocycle directly from the isodiazene was prohibitively high in energy (20.8 kcal/mol via ***cis*-TS-1** vs 16.9 kcal/mol via ***trans*-TS-1**, Figure S10). Collectively, these calculations invalidate our hypothesis for central-helical-central chirality transfer via the spiro intermediate **II**. Rather, our calculations predict that complete racemization of intermediate **II** should occur prior to the rearrangement to the indane, which is inconsistent with our experimental data.

Two Mechanisms Hypothesis. Having discarded the helical chirality hypothesis, we next considered experiments that would probe whether the isodiazene proceeds via multiple competing intermediates. Accordingly, we conducted the deuterium-labeling experiment with the isotopomer 4,4-d_2-**1a** to form d_2-**3a** (Figure 8). In the event, we observed that the

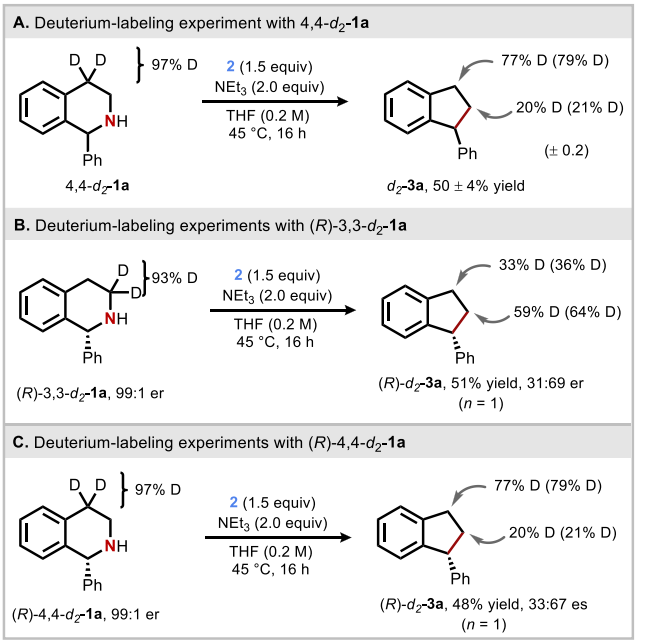

Figure 8. Alternate isotope labeling experiment and simultaneous deuterium-labeling and enantiospecificity experiments.

isotope scrambling ratio was significantly changed from 36:64 (in 3,3-d_2-**1a**, Figure 4A) to 21:79 (Figure 8A). Because one

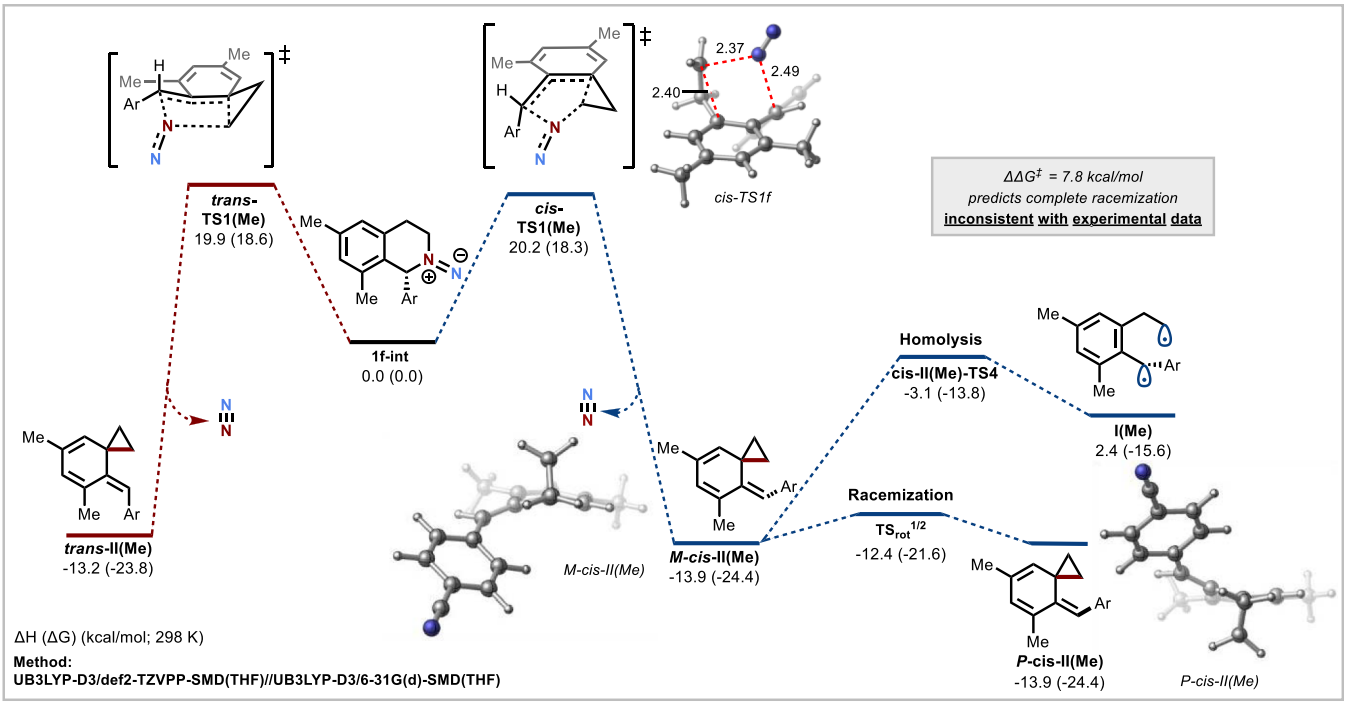

Figure 7. Interrogating a scenario involving a putatively helically chiral cis-spirocyclopropane intermediate. Corrections to the single-point energies for the open-shell singlet geometries were made with the Yamaguchi correction (Tables S3 and S4).

https://doi.org/10.1021/jacs.4c02491
J. Am. Chem. Soc. 2024, 146, 17719−17727

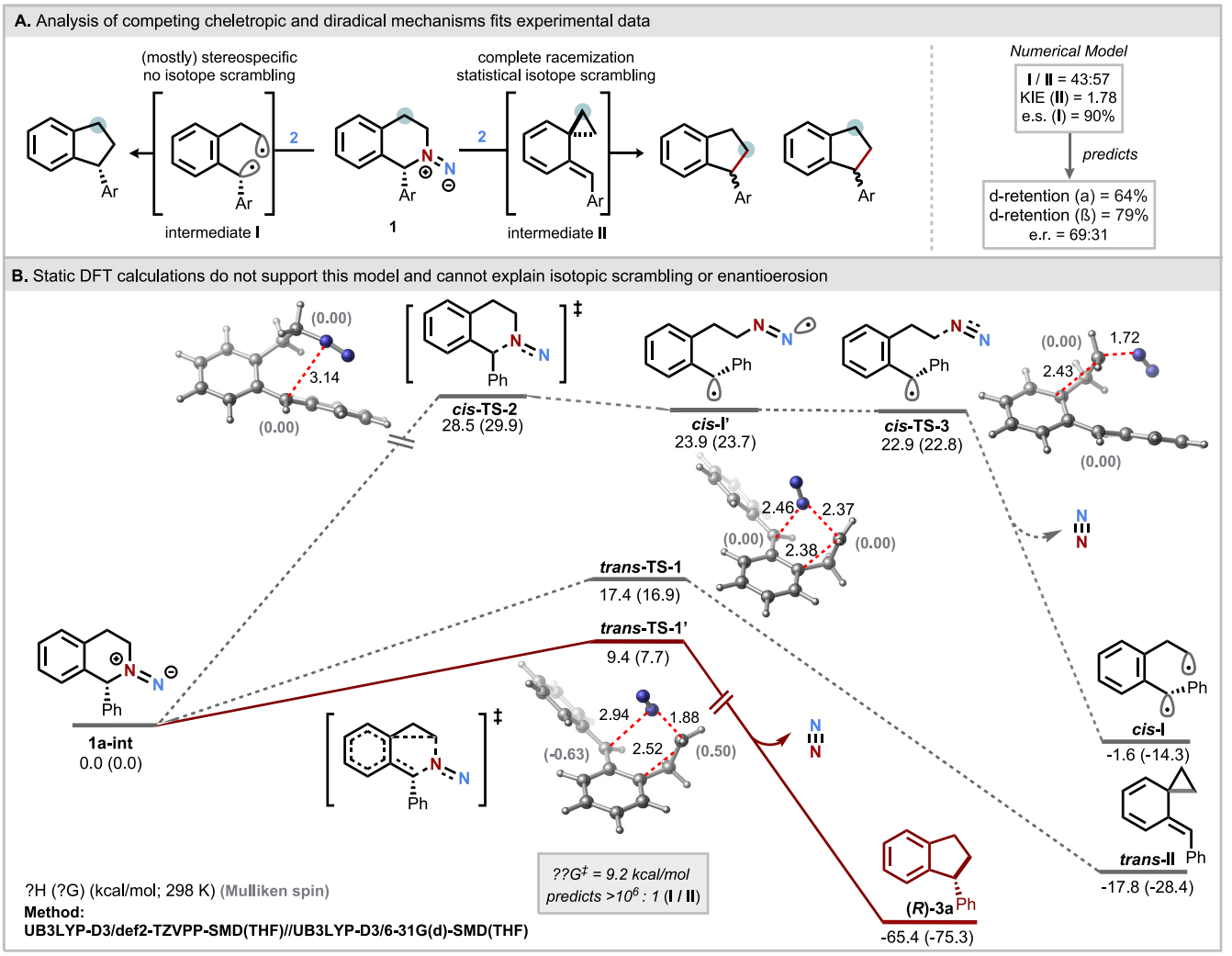

Figure 9. Interrogating a scenario involving competing diradical and cheletropic mechanisms. $\Delta\Delta G$ is the energetic difference between open-shell singlet ***trans*-TS-1′** and closed-shell ***trans*-TS-1** computed using UB3LYP-D3/6-31G(*d*)-SMF(THF) and RB3LYP-D3/6-31G(*d*)-SMF(THF), respectively. Corrections to the single-point energies for the open-shell singlet geometries were made with the Yamaguchi correction (Tables S3 and S4).

intermediate cannot have two different KIEs, this immediately necessitates the consideration of a second pathway in competition with the formation of *trans*-**II**. To gain clarity on this result, we prepared the enantiopure *and* deuterium-labeled substrates (*R*)-3,3-d_2-**1a** and (*R*)-4,4-d_2-**1a** (Figure 8B,C). Upon subjection to the reaction, the enantiospecificities were not significantly impacted by deuterium substitution, and similarly the deuterium scrambling ratios were not significantly affected by enantioenrichment. These results suggest that the mechanism by which memory of chirality occurs is decoupled from isotopic scrambling.

One can construct a numerical model that captures these experimental results with two competitive mechanisms, one involving the diradical **I** and the other involving spirocycle **II** (Figure 9A). Intermediate **I** would preclude isotope scrambling and proceed with some degree of stereospecificity, while intermediate **II** should lead to complete racemization and near-complete scrambling, with a 2° KIE favoring migration of the unlabeled carbon due to hybridization changes. A system of three equations in three unknowns built on these assumptions predicts that the isodiazene partitions 43:57 to **I** and **II**, respectively, with a KIE of 1.71 for the rearrangement of intermediate **II** and 88% enantiospecificity from intermediate **I** (see Section 4 of the Supporting Information).

Unfortunately, DFT calculations starting from the putative isodiazene intermediate **1a-int** were also inconsistent with this model (Figure 9B).[41] Specifically, two *structurally* similar transition states could be found but with divergent outcomes and significantly different energetics. The higher energy transition state ***trans*-TS-1** ($\Delta G^{\ddagger}$ = 16.9 kcal/mol), a restricted singlet, corresponds to a concerted cheletropic N_2 extrusion affording the vinyl cyclopropane intermediate ***trans*-II**. In contrast, the lower energy, open-shell singlet transition state ***trans*-TS-1′** ($\Delta G^{\ddagger}$ = 7.7 kcal/mol) exhibits much longer C−N (2.94 vs 2.46 Å) and C−C (2.52 vs 2.38 Å) bonds. Unexpectedly, optimization of the end point of intrinsic reaction coordinate (IRC) for this transition state provided the stereoretentive product (*R*)-**3a** directly (i.e., without formation of a diradical intermediate along the IRC), suggesting a direct coupling pathway (Figure S7). Though this latter pathway could in principle *function* in an analogous fashion to intermediate **I**, the predicted energy difference between these two transition states ($\Delta\Delta G^{\ddagger}$ = 9.2 kcal/mol) is inconsistent

https://doi.org/10.1021/jacs.4c02491
J. Am. Chem. Soc. 2024, 146, 17719−17727

with the 43:57 partitioning ratio modeled from the experimental results.

Moreover, it was unclear how enantioerosion might arise in a direct coupling with no discrete diradical. The stepwise homolysis (via **cis-TS-2**) of the weaker benzylic C−N bond (to form diradical **I′**) was ruled out (>10 kcal/mol above either competing mechanism).

Dynamic Effects. These inconsistencies prompted us to consider dynamic effects as a possible explanation.[42−47] Such dynamic effects have been well documented in related 1,4-diradical systems, but 1,5-diradicals have been comparatively understudied.[48−57] Given the relatively flat surface and similarity of structures along the IRC to diradical intermediates, we considered that dynamic effects from an open-shell, asynchronous N_2 extrusion (i.e., an non-IRC pathway via a potential entropic diradical intermediate) could explain the experimental results.

To explore this mechanistic possibility, we performed quasi-classical molecular dynamics simulations using Progdyn from ***trans*-TS-1′** toward the direction of the products at 300 K over 2000 fs with a time step of 1 fs (Figure 10) (see the Supporting Information for details). Overall, in contrast to static DFT calculations, these dynamic simulations led to four main outcomes: (i) spirocycle **II** (6%), (ii) entropic intermediate diradical **I** (46%),[45,58−63] (iii) (*S*)-**3a** (*inversion*, 21%), and (iv) the (*R*)-**3a** IRC product (*retention*, 26%). Notably, from ***trans*-TS-1′**, the majority of trajectories (73%) proceed along a non-IRC pathway, leading to the formation of (i)−(iii).

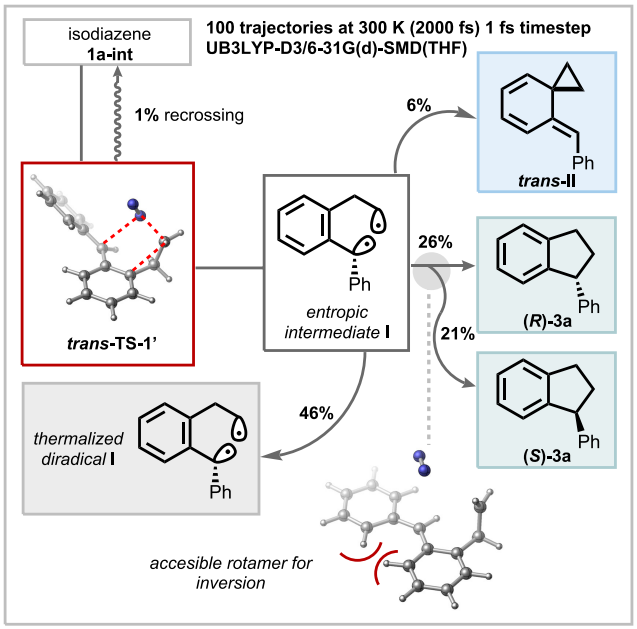

Figure 10. Dynamic effects indicate the formation of both 1,3- and 1,5-coupling products from a single transition state and explain the observed nonstatistical product distribution.

We also investigated classical dynamics of ***trans*-TS-1′** with a more robust and computationally intensive Born−Oppenheimer molecular dynamics[64] (BOMD, see the Supporting Information for details) employing the canonical (*N*, *V*, *E*) ensemble. BOMD affords very similar results to Progdyn (within ∼2% of original predictions) with the notable exception that it predicts the formation of a high-energy spirodiazene intermediate (*P*/*M*-*trans*-**III**, Figure S20) instead of the thermalized diradical **I**. DFT calculations predict that C−N bond homolysis from *P*/*M*-*trans*-**III** would occur with a barrier of ∼8 kcal/mol to generate a diazenyl diradical (*P*/*M*-*trans*-**I′** via *P*/*M*-*trans*-*TS*-*6*, Figure S21). The formation of the thermalized diradical **I** would then occur by stepwise homolysis with an insignificant barrier of 0.7 kcal/mol (*P*/*M*-*trans*-*TS*-*3*, Figure S21).

As the barrier for the alternative mechanism via ***cis*-TS-1′** was significantly higher in energy (∼2 kcal/mol), the products from the dynamic simulations from this competing transition state are not expected to contribute significantly to the overall product distribution (see Figure S14 for further details). Though these combined trajectories are not in perfect numerical agreement with the experimental results, the prediction of the spirocyclopropane intermediate **II** as a competitive pathway is far more consistent than the $>10^6$:1 ratio suggested by static DFT, and the identification of a dynamically accessible inversion pathway via **I** is likewise more consistent than the purely stereospecific direct coupling predicted by static DFT.

In the 8-methyl-substituted analogue (**1f-int**), the concerted cheletropic N_2 extrusions [affording the vinyl cyclopropane intermediates ***trans*-II(Me)** and ***cis*-II(Me)**, via ***trans*-TS-1(Me)** and ***cis*-TS-1(Me)**, respectively] were once again higher in energy than the open shell transition states ***trans*-TS-1′(Me)** and ***cis*-TS-1′(Me)**. Additionally, ***trans*-TS-1′(Me)** exhibited much longer C−N (3.08 vs 2.46 Å) and C−C (2.52 vs 2.38 Å) bond lengths than ***trans*-TS-1(Me)** with an increase in the magnitude of Mulliken spin at the site of C−N bond cleavage (Figure S11). Contrary to **1a-int**, the open-shell singlet transition states ***trans*-TS-1′(Me)** ($\Delta G^{\ddagger}$ = 8.5 kcal/mol) and ***cis*-TS-1′(Me)** ($\Delta G^{\ddagger}$ = 8.9 kcal/mol) are nearly identical in energy. Once again, the optimization of the end point of the IRC calculations for transition states ***trans*-TS-1′(Me)** and ***cis*-TS-1′(Me)** (Figures S8 and S11) provided the stereoretentive product (*R*)-**3f** directly. Accordingly, analogous quasi-classical molecular dynamics simulations were propagated from the isoenergetic transition states ***trans*-TS-1′(Me)** and ***cis*-TS-1′(Me)** (Figure 11, for additional details, see Figure S17). In both cases, the only indane product observed was the retention product (*R*)-**3f** (91 and 57% of trajectories, respectively). Additionally, no 1,3-coupling trajectories were observed starting from either transition state, consistent with the minimal isotopic scrambling observed in 3,3-d_2-**1f**.

Comparison of the mechanism of inversion starting from ***trans*-TS-1′** and ***trans*-TS-1′(Me)** reveals a *dynamic maintenance of helical chirality* which manifests through torsional strain in the latter trajectories rather than via a helically chiral spirocyclic intermediate as originally proposed above. This torsional strain prevents the aryl group from rotating past the 8-methyl substituent and thus enforces enantiospecificity.[65−67] Moreover, this same torsional effect also prevents the 1,3-coupling from occurring and substantially decreases the lifetime of the diradical (6% compared to 46% remaining at 2000 fs).

In conclusion, we have provided evidence for the formation of a dearomatized spirocycle intermediate in the nitrogen deletion reaction of tetrahydroisoquinolines through a combination of enantiospecificity measurements, isotope-labeling experiments, and quantum mechanical calculations, as well as by analogy to isolable analogues formed from heterocyclic variants of this scaffold. A unified model involving dynamically controlled partitioning between this unusual

https://doi.org/10.1021/jacs.4c02491
J. Am. Chem. Soc. 2024, 146, 17719−17727

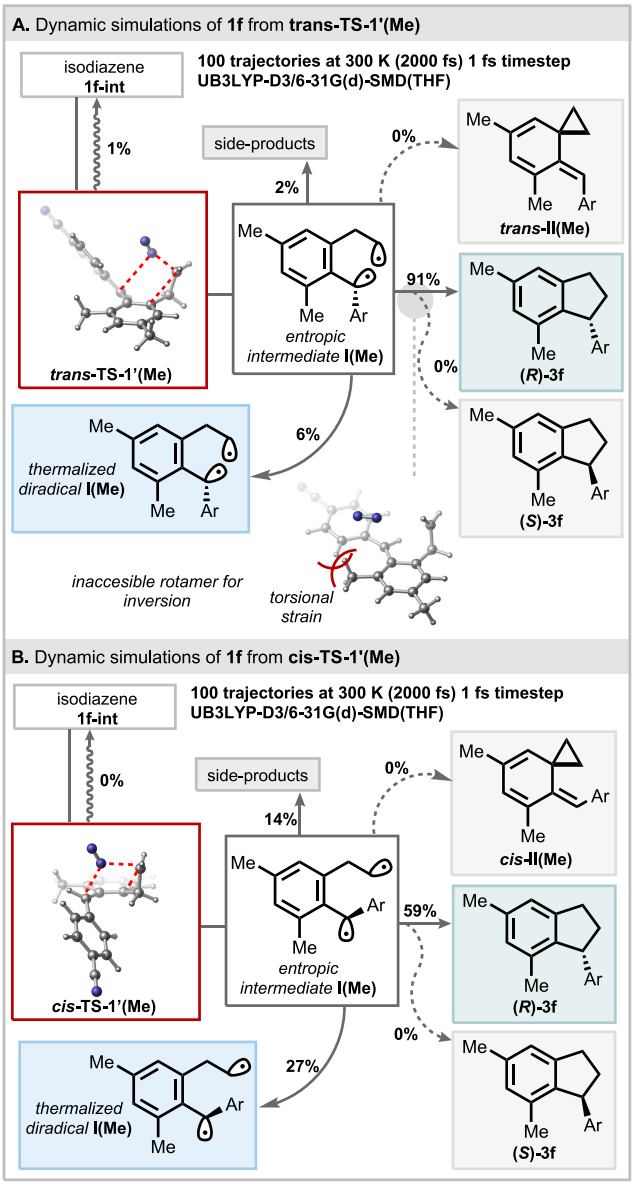

Figure 11. Dynamics of **1f** isodiazene reveal retention of stereochemistry through torsional control.

spirocycle and the traditional diradical mechanism, with torsional control of diradical dynamics influencing stereospecificity is proposed to explain the nonstatistical experimental results. This study adds to the growing body of understanding concerning the reactivity of isodiazenes and showcases a practical application of molecular dynamics in elucidating complex reaction mechanisms for which static DFT fails.

■ ASSOCIATED CONTENT

Supporting Information

The Supporting Information is available free of charge at https://pubs.acs.org/doi/10.1021/jacs.4c02491.

Experimental procedures, supporting characterization data and spectra, computational procedures, and coordinates (PDF)

■ AUTHOR INFORMATION

Corresponding Authors

Osvaldo Gutierrez − *Department of Chemistry, Texas A&M University, College Station, Texas 77843, United States;* orcid.org/0000-0001-8151-7519; Email: og.labs@tamu.edu

Mark D. Levin − *Department of Chemistry, University of Chicago, Chicago, Illinois 60637, United States;* orcid.org/0000-0002-4461-363X; Email: marklevin@uchicago.edu

Authors

Jeanne Masson-Makdissi − *Department of Chemistry, University of Chicago, Chicago, Illinois 60637, United States*

Remy F. Lalisse − *Department of Chemistry, Texas A&M University, College Station, Texas 77843, United States;* orcid.org/0000-0002-4556-5641

Mingbin Yuan − *Department of Chemistry and Biochemistry, University of Maryland, College Park, Maryland 20742, United States*

Balu D. Dherange − *Department of Chemistry, University of Chicago, Chicago, Illinois 60637, United States;* orcid.org/0000-0002-4123-5012

Complete contact information is available at: https://pubs.acs.org/10.1021/jacs.4c02491

Author Contributions

‖J.M.-M., R.F.L. and M.Y. contributed equally to this work.

Funding

M.D.L. thanks the NSF CAREER (CHE-2235826) for funding. O.G. acknowledges the National Institutes of Health (R35GM137797), Camille and Henry Dreyfus Foundation, and the Welch Foundation (A-2102-20220331) for funding, and Texas A&M University HPRC resources (https://hprc.tamu.edu) for computational resources.

Notes

The authors declare no competing financial interest.

■ ACKNOWLEDGMENTS

We thank Dr. Sean H. Kennedy (UChicago) for initial investigations into this phenomenon. We thank Patrick Kelly (UChicago), Yahia Ali (UChicago), Prof. Viresh Rawal (UChicago), Dr. James B. Gerken (UW Madison), and Prof. Dan Singleton (TAMU) for helpful discussions. We thank the Dong and Rawal laboratories for generously lending chemicals.

■ REFERENCES

(1) Kennedy, S. H.; Dherange, B. D.; Berger, K. J.; Levin, M. D. Skeletal Editing through Direct Nitrogen Deletion of Secondary Amines. *Nature* **2021**, *593* (7858), 223−227.

(2) Zou, X.; Zou, J.; Yang, L.; Li, G.; Lu, H. Thermal Rearrangement of Sulfamoyl Azides: Reactivity and Mechanistic Study. *J. Org. Chem.* **2017**, *82* (9), 4677−4688.

(3) Qin, H.; Cai, W.; Wang, S.; Guo, T.; Li, G.; Lu, H. N-Atom Deletion in Nitrogen Heterocycles. *Angew. Chem., Int. Ed.* **2021**, *60* (38), 20678−20683.

(4) Hui, C.; Brieger, L.; Strohmann, C.; Antonchick, A. P. Stereoselective Synthesis of Cyclobutanes by Contraction of Pyrrolidines. *J. Am. Chem. Soc.* **2021**, *143*, 18864−18870.

(5) Berger, K. J.; Driscoll, J. L.; Yuan, M.; Dherange, B. D.; Gutierrez, O.; Levin, M. D. Direct Deamination of Primary Amines via Isodiazene Intermediates. *J. Am. Chem. Soc.* **2021**, *143* (42), 17366−17373.

(6) Dherange, B. D.; Yuan, M.; Kelly, C. B.; Reiher, C. A.; Grosanu, C.; Berger, K. J.; Gutierrez, O.; Levin, M. D. Direct Deaminative Functionalization. *J. Am. Chem. Soc.* **2023**, *145* (1), 17−24.
(7) Holovach, S.; Melnykov, K. P.; Poroshyn, I.; Iminov, R. T.; Dudenko, D.; Kondratov, I.; Levin, M.; Grygorenko, O. O. C-C Coupling through Nitrogen Deletion: Application to Library Synthesis. *Chem.—Eur. J.* **2023**, *29* (4), No. e202203470.
(8) Steiniger, K. A.; Lamb, M. C.; Lambert, T. H. Cross-Coupling of Amines via Photocatalytic Denitrogenation of In Situ Generated Diazenes. *J. Am. Chem. Soc.* **2023**, *145* (21), 11524−11529.
(9) Chattapadhyay, D.; Aydogan, A.; Doktor, K.; Maity, A.; Wu, J. W.; Michaudel, Q. Harnessing Sulfur(VI) Fluoride Exchange Click Chemistry and Photocatalysis for Deaminative Benzylic Arylation. *ACS Catal.* **2023**, *13* (11), 7263−7268.
(10) Schultz, P. G.; Dervan, P. B. Synthesis and Direct Spectroscopic Observation of N-(2,2,5,5-Tetramethylpyrrolidinyl)Nitrene. Comparison of Five- and Six-Membered Cyclic 1,1-Dialkyldiazenes. *J. Am. Chem. Soc.* **1980**, *102* (2), 878−880.
(11) Schultz, P. G.; Dervan, P. B. Photochemistry of a 1,1-Diazene, N-(2,2,5,5-Tetramethylpyrrolidinyl)Nitrene. *J. Am. Chem. Soc.* **1981**, *103* (6), 1563−1564.
(12) Schultz, P. G.; Dervan, P. B. Photochemistry of 1,1-Diazenes. Direct and Sensitized Photolyses of N-(2,2,5,5-Tetramethylpyrrolidyl)Nitrene, Dl-N-(2,5-Diethyl-2,5-Dimethylpyrrolidyl)Nitrene, and N-(2,2,6,6-Tetramethylpiperidyl)-Nitrene. *J. Am. Chem. Soc.* **1982**, *104* (24), 6660−6668.
(13) McIntyre, D. K.; Dervan, P. B. 1,1-Di-Tert-Butyldiazene. *J. Am. Chem. Soc.* **1982**, *104* (23), 6466−6468.
(14) Hinsberg, W. D.; Schultz, P. G.; Dervan, P. B. Direct Studies of 1,1-Diazenes. Syntheses, Infrared and Electronic Spectra, and Kinetics of the Thermal Decomposition of N-(2,2,6,6-Tetramethylpiperidyl)-Nitrene and N-(2,2,5,5-Tetramethylpyrrolidyl)Nitrene. *J. Am. Chem. Soc.* **1982**, *104* (3), 766−773.
(15) Hinsberg, W. D.; Dervan, P. B. Synthesis and Direct Spectroscopic Observation of a 1,1-Dialkyldiazene. Infrared and Electronic Spectrum of N-(2,2,6,6-Tetramethylpiperidyl)Nitrene. *J. Am. Chem. Soc.* **1978**, *100* (5), 1608−1610.
(16) Hinsberg, W. D.; Dervan, P. B. Kinetics of the Thermal Decomposition of a 1,1-Dialkyldiazene, N-(2,2,6,6-Tetramethylpiperidyl)Nitrene. *J. Am. Chem. Soc.* **1979**, *101* (20), 6142−6144.
(17) Duan, D. C.; Dervan, P. B. Evidence for a Stereospecific 1,2-Elimination Reaction in a 1,1-Diazene. Synthesis and Decomposition of [N-Phenyl(Threo- and Erythro)-2-Deuterio-1-Methylpropyl)-Amino]Nitrene. *J. Org. Chem.* **1983**, *48* (7), 970−976.
(18) Dervan, P. B.; Squillacote, M. E.; Lahti, P. M.; Sylwester, A. P.; Roberts, J. D. Nitrogen-15 NMR Spectrum of a 1,1-Diazene. N-(2,2,6,6-Tetramethylpiperidyl)Nitrene. *J. Am. Chem. Soc.* **1981**, *103* (5), 1120−1122.
(19) Dervan, P. B.; Uyehara, T. Stereochemical Tests of Cyclic 1,1-Dialkyldiazene Fragmentation Reactions. Thermal Decomposition of N-(Cis-(and Trans-)2,3-(and 2,5-)Dimethylpyrrolidine)Nitrenes. *J. Am. Chem. Soc.* **1979**, *101* (8), 2076−2082.
(20) Miller, R. D.; Golitz, P.; Janssen, J.; Lemmens, J. Alternative Precursors to 1,4-Acyl Alkyl Biradicals: Cyclic N-Acyl-1,1-Diazenes. *J. Am. Chem. Soc.* **1984**, *106* (23), 7277−7279.
(21) Lemal, D. M.; Rave, T. W. Diazenes from Angeli's Salt. *J. Am. Chem. Soc.* **1965**, *87* (2), 393−394.
(22) Lemal, D. M.; Menger, F.; Coats, E. The Diazene-Hydrazone Rearrangement. *J. Am. Chem. Soc.* **1964**, *86* (12), 2395−2401.
(23) Jurczyk, J.; Lux, M. C.; Adpressa, D.; Kim, S. F.; Lam, Y.; Yeung, C. S.; Sarpong, R. Photomediated Ring Contraction of Saturated Heterocycles. *Science* **2021**, *373* (6558), 1004−1012.
(24) Shen, L.; Lin, Z.; Guo, B.; Zi, W. Synthesis of Cycloheptanoids through Catalytic Enantioselective (4 + 3)-Cycloadditions of 2-Aminoallyl Cations with Dienol Silyl Ethers. *Nat. Synth.* **2022**, *1* (11), 883−891.
(25) Mansson, C. M. F.; Burns, N. Z. Aqueous Amine-Tolerant [2 + 2] Photocycloadditions of Unactivated Olefins. *J. Am. Chem. Soc.* **2022**, *144* (43), 19689−19694.
(26) Wright, B. A.; Matviitsuk, A.; Black, M. J.; García-Reynaga, P.; Hanna, L. E.; Herrmann, A. T.; Ameriks, M. K.; Sarpong, R.; Lebold, T. P. Skeletal Editing Approach to Bridge-Functionalized Bicyclo[1.1.1]Pentanes from Azabicyclo[2.1.1]Hexanes. *J. Am. Chem. Soc.* **2023**, *145* (20), 10960−10966.
(27) We previously identified an analogous 1,3-coupling product in the N-deletion of anatabine, a tetrahydropyridine-containing alkaloid. However, even in that case, it was formed in competition with the expected 1,5-coupling product—the observation of exclusive cyclopropane formation in a system that breaks antiaromaticity to do so was quite unexpected.
(28) Houk, K. N.; Nendel, M.; Wiest, O.; Storer, J. W. The Vinylcyclopropane-Cyclopentene Rearrangement: A Prototype Thermal Rearrangement Involving Competing Diradical Concerted and Stepwise Mechanisms. *J. Am. Chem. Soc.* **1997**, *119* (43), 10545−10546.
(29) Nendel, M.; Sperling, D.; Wiest, O.; Houk, K. N. Computational Explorations of Vinylcyclopropane-Cyclopentene Rearrangements and Competing Diradical Stereoisomerizations. *J. Org. Chem.* **2000**, *65* (11), 3259−3268.
(30) Wellington, C. A. The thermal isomerization of vinylcyclopropane. *J. Phys. Chem.* **1962**, *66* (9), 1671−1674.
(31) Hudlicky, T.; Reed, J. W. From Discovery to Application: 50 Years of the Vinylcyclopropane-Cyclopentene Rearrangement and Its Impact on the Synthesis of Natural Products. *Angew. Chem., Int. Ed.* **2010**, *49* (29), 4864−4876.
(32) Neureiter, N. Notes- Pyrolysis of 1,1-Dichloro-2-Vinylcyclopropane Synthesis Of2-Chlorocyclopentadiene. *J. Org. Chem.* **1959**, *24* (12), 2044−2046.
(33) Trost, B. M.; Keeley, D. E. New Synthetic Methods. A Stereocontrolled Approach to Cyclopentane Annelation. *J. Am. Chem. Soc.* **1976**, *98* (1), 248−250.
(34) Danheiser, R. L.; Martinez-Davila, C.; Morin, J. M., Jr. Synthesis of 3-Cyclopentenols by Alkoxy-Accelerated Vinylcyclopropane Rearrangement. *J. Org. Chem.* **1980**, *45* (7), 1340−1341.
(35) Hudlicky, T.; Heard, N. E.; Fleming, A. 4-Siloxy-.Alpha.-Bromocrotonate: A New Reagent for [2 + 3] Annulation Leading to Oxygenated Cyclopentenes at Low Temperatures. *J. Org. Chem.* **1990**, *55* (9), 2570−2572.
(36) Baldwin, J. E.; Villarica, K. A.; Freedberg, D. I.; Anet, F. A. L. Stereochemistry of the Thermal Isomerization of Vinylcyclopropane to Cyclopentene. *J. Am. Chem. Soc.* **1994**, *116* (23), 10845−10846.
(37) Alezra, V.; Kawabata, T. Recent Progress in Memory Of Chirality (MOC): An Advanced Chiral Pool. *Synthesis* **2016**, *48* (18), 2997−3016.
(38) Kawabata, T.; Suzuki, H.; Nagae, Y.; Fuji, K. A Chiral Nonracemic Enolate with Dynamic Axial Chirality: Direct Asymmetric α-Methylation of α-Amino Acid Derivatives. *Angew. Chem., Int. Ed.* **2000**, *39* (12), 2155−2157.
(39) Gauvreau, D.; Barriault, L. Conservation of the Planar Chiral Information in the Tandem Oxy-Cope/Ene Reaction. *J. Org. Chem.* **2005**, *70* (4), 1382−1388.
(40) Hoffmann, R. W. Allylic 1,3-Strain as a Controlling Factor in Stereoselective Transformations. *Chem. Rev.* **1989**, *89* (8), 1841−1860.
(41) Both singlet and triplet surface pathways were considered, as well as crossing between the two surfaces. For the sake of simplicity, only the lower energy singlet pathway is discussed.
(42) Carpenter, B. K. Dynamic Behavior of Organic Reactive Intermediates. *Angew. Chem., Int. Ed.* **1998**, *37* (24), 3340−3350.
(43) Doubleday, C. Mechanism of the Vinylcyclopropane-Cyclopentene Rearrangement Studied by Quasiclassical Direct Dynamics. *J. Phys. Chem. A* **2001**, *105* (26), 6333−6341.
(44) Hong, Y. J.; Tantillo, D. J. A Potential Energy Surface Bifurcation in Terpene Biosynthesis. *Nat. Chem.* **2009**, *1* (5), 384−389.

https://doi.org/10.1021/jacs.4c02491
J. Am. Chem. Soc. 2024, 146, 17719−17727

(45) Yang, Z.; Jamieson, C. S.; Xue, X.-S.; Garcia-Borràs, M.; Benton, T.; Dong, X.; Liu, F.; Houk, K. N. Mechanisms and Dynamics of Reactions Involving Entropic Intermediates. *Trends Chem.* **2019**, *1* (1), 22−34.
(46) Roytman, V. A.; Jin, S.; Nguyen, V. T.; Nguyen, V. D.; Haug, G. C.; Larionov, O. V.; Singleton, D. A. Bond Memory in Dynamically Determined Stereoselectivity. *J. Am. Chem. Soc.* **2020**, *142* (1), 85−88.
(47) Feng, Z.; Guo, W.; Kong, W.-Y.; Chen, D.; Wang, S.; Tantillo, D. J. Analogies between Photochemical Reactions and Ground-State Post-Transition-State Bifurcations Shed Light on Dynamical Origins of Selectivity. *Nat. Chem.* **2024**, *16*, 615−623.
(48) Biellmann, J. F.; Ducep, J. B.; Vicens, J. J. Rearrangement of Carbanions and of Ylides Derived from 4-Thiacyclohexenyl Systems. *Tetrahedron* **1976**, *32* (14), 1801−1805.
(49) Padwa, A.; Ku, H. Intramolecular Cycloaddition Reactions of Olefinic Tosylhydrazones. *J. Org. Chem.* **1980**, *45* (19), 3756−3766.
(50) Padwa, A.; Chou, C. S. Effects of Substituents on the Type II Photoreaction of Tetrasubstituted Cyclopropenes. *Tetrahedron* **1981**, *37* (19), 3269−3274.
(51) Kaupp, G.; Zimmermann, I. First Detection of a π-Coupled 1,5-Diradical via Cycloaddition. *Angew. Chem., Int. Ed. Engl.* **1981**, *20* (12), 1018−1019.
(52) Wilson, R. M.; Rekers, J. W. The Decomposition of Bicyclic Endoperoxides: An Isomorphous Synthesis of Frontalin via 1,5-Dimethyl-6,7-Dioxabicyclo[3.2.1]Octane. *J. Am. Chem. Soc.* **1981**, *103* (1), 206−207.
(53) Uyehara, T.; Takahashi, M.; Kato, T. Sulfide Extrusion from the Methylsulfonium Salts of 8-Thiabicyclo [3.2.1]Oct-2-Enes and the Related Sulfonium Salts by Methyllithium. *Tetrahedron Lett.* **1984**, *25* (36), 3999−4002.
(54) Ikeda, H.; Hoshi, Y.; Miyashi, T. 1,3-Bis(4-Methoxyphenyl)-Cyclohexane-1,3-Diyl Cation Radical: Divergent Reactivity Depending upon Electron-Transfer Conditions. *Tetrahedron Lett.* **2001**, *42* (48), 8485−8488.
(55) Merkley, N.; Reid, D. L.; Warkentin, J. Remarkable Aromatic Substitution by a 1,5-Diradical. *Tetrahedron Lett.* **2002**, *43* (11), 1927−1929.
(56) Abe, M. Diradicals. *Chem. Rev.* **2013**, *113* (9), 7011−7088.
(57) Dotson, J. J.; Liepuoniute, I.; Bachman, J. L.; Hipwell, V. M.; Khan, S. I.; Houk, K. N.; Garg, N. K.; Garcia-Garibay, M. A. Taming Radical Pairs in the Crystalline Solid State: Discovery and Total Synthesis of Psychotriadine. *J. Am. Chem. Soc.* **2021**, *143* (10), 4043−4054.
(58) Gonzalez-James, O. M.; Kwan, E. E.; Singleton, D. A. Entropic Intermediates and Hidden Rate-Limiting Steps in Seemingly Concerted Cycloadditions. Observation, Prediction, and Origin of an Isotope Effect on Recrossing. *J. Am. Chem. Soc.* **2012**, *134* (4), 1914−1917.
(59) Black, K.; Liu, P.; Xu, L.; Doubleday, C.; Houk, K. N. Dynamics, Transition States, and Timing of Bond Formation in Diels-Alder Reactions. *Proc. Natl. Acad. Sci. U.S.A.* **2012**, *109* (32), 12860−12865.
(60) Yang, Z.; Yu, P.; Houk, K. N. Molecular Dynamics of Dimethyldioxirane C-H Oxidation. *J. Am. Chem. Soc.* **2016**, *138* (12), 4237−4242.
(61) Carlsen, R.; Wohlgemuth, N.; Carlson, L.; Ess, D. H. Dynamical Mechanism May Avoid High-Oxidation State Ir(V)-H Intermediate and Coordination Complex in Alkane and Arene C-H Activation by Cationic Ir(III) Phosphine. *J. Am. Chem. Soc.* **2018**, *140* (35), 11039−11045.
(62) Joy, J.; Ess, D. H. Direct Dynamics Trajectories Demonstrate Dynamic Matching and Nonstatistical Radical Pair Intermediates during Fe-Oxo-Mediated C-H Functionalization Reactions. *J. Am. Chem. Soc.* **2023**, *145* (13), 7628−7637.
(63) Zhang, Y.; Cao, C.; She, Y.; Yang, Y.-F.; Houk, K. N. Molecular Dynamics of Iron Porphyrin-Catalyzed C-H Hydroxylation of Ethylbenzene. *J. Am. Chem. Soc.* **2023**, *145* (26), 14446−14455.
(64) Schlegel, H. B.; Iyengar, S. S.; Li, X.; Millam, J. M.; Voth, G. A.; Scuseria, G. E.; Frisch, M. J. Ab Initio Molecular Dynamics: Propagating the Density Matrix with Gaussian Orbitals. III. Comparison with Born-Oppenheimer Dynamics. *J. Chem. Phys.* **2002**, *117* (19), 8694−8704.
(65) von Rague Schleyer, P. Torsional Effects in Polycyclic Systems. II. The Stereochemistry of Attack and Departure in Norbornane Derivatives. *J. Am. Chem. Soc.* **1967**, *89* (3), 701−703.
(66) Martinelli, M. J.; Peterson, B. C.; Khau, V. V.; Hutchison, D. R.; Leanna, M. R.; Audia, J. E.; Droste, J. J.; Wu, Y.-D.; Houk, K. N. Stereoselective Epoxidations and Electrophilic Additions to Partial Ergot Alkaloids and Conformationally-Fixed Styrenes. Experimental and Theoretical Modeling Evidence for the Importance of Torsional Steering as a Stereocontrol Element. *J. Org. Chem.* **1994**, *59* (8), 2204−2210.
(67) Cheong, P. H.-Y.; Yun, H.; Danishefsky, S. J.; Houk, K. N. Torsional Steering Controls the Stereoselectivity of Epoxidation in the Guanacastepene A Synthesis. *Org. Lett.* **2006**, *8* (8), 1513−1516.

https://doi.org/10.1021/jacs.4c02491
J. Am. Chem. Soc. 2024, 146, 17719−17727